Research Article Open Access

Ziming Xiong, Mingyang Wang, ShaoShuai Shi*, YuanPu Xia, Hao Lu, and Lin Bu

Water Inrush Analysis of the Longmen Mountain Tunnel Based on a 3D Simulation of the Discrete Fracture Network

https://doi.org/10.1515/geo-2017-0049
Received February 7, 2017; accepted August 23, 2017

Abstract: The construction of tunnels and underground engineering in China has developed rapidly in recent years in both the number and the length of tunnels. However, with the development of tunnel construction technology, risk assessment of the tunnels has become increasingly important. Water inrush is one of the most important causes of engineering accidents worldwide, resulting in considerable economic and environmental losses. Accordingly, water inrush prediction is important for ensuring the safety of tunnel construction. Therefore, in this study, we constructed a three-dimensional discrete network fracture model using the Monte Carlo method first with the basic data from the engineering geological map of the Longmen Mountain area, the location of the Longmen Mountain tunnel. Subsequently, we transformed the discrete fracture networks into a pipe network model. Next, the DEM of the study area was analysed and a submerged analysis was conducted to determine the water storage area. Finally, we attempted to predict the water inrush along the Longmen Mountain tunnel based on the Darcy flow equation. Based on the contrast of water inrush between the proposed approach, groundwater dynamics and precipitation infiltration method, we conclude the following: the water inflow determined using the groundwater dynamics simulation results are basically consistent with those in the D2K91+020 to D2K110+150 mileage. Specifically, in the D2K91+020 to D2K94+060, D2K96+440 to D2K98+100 and other sections of the tunnel, the simulated and measured results are in close agreement and show that this method is effective. In general, we can predict the water inflow in the area of the Longmen Mountain tunnel based on the existing fracture joint parameters and the hydrogeological data of the Longmen Mountain area, providing a water inrush simulation and guiding the tunnel excavation and construction stages.

Keywords: Three-dimensional geological model; Monte Carlo method; Discrete fracture networks; Longmen Mountain tunnel; Water inrush

1 Introduction

In the process of tunnel construction, the primary problem to be considered is construction safety. A variety of natural disasters can occur during tunnel construction [1, 2]. The water inrush is one of the primary concern problems that a large number of hazards of water inrush have occurred during the construction of tunnel at home and abroad and has caused serious economic losses, project delays, environmental destruction and other problems [3–6]. Therefore, the risk assessment and control of water inrush have become the key technical concerns in tunnel construction. The prediction of water inrush in tunnel can take two forms: prediction before excavation or predicting the process during tunnel excavation. They are the risk assessment at different stage of tunnel construction. The former is the foundation of the latter prediction research. So the prediction before excavation is very important for the risk analysis of water inrush. The direction and quantity of water in the tunnel site is the main factor for the water inrush evaluation. So the present article through the direc-

***Corresponding Author: ShaoShuai Shi:** Geotechnical and Structural Engineering Research Center, Shandong University, Jinan, China, E-mail address: shishaoshuai@sdu.edu.cn
State Key Laboratory for Geomechanics and Deep Underground Engineering, China University of Mining and Technology, Xuzhou, China
Ziming Xiong, Mingyang Wang: College of Mechanical Engineering, Nanjing University of Science and Technology; State Key Laboratory of Disaster Prevention and Mitigation of Explosion and Impact, Army Engineering University of PLA
YuanPu Xia, Hao Lu: State Key Laboratory of Disaster Prevention and Mitigation of Explosion and Impact, Army Engineering University of PLA
Lin Bu: Geotechnical and Structural Engineering Research Center, Shandong University

tion of water flow and the quantity of water to predict the water inrush risk before tunnel excavation. The experience analytical method such as the water balance method and the groundwater dynamics method, is the most commonly used method for the prediction of the water inflow in the tunnel before excavation [7]. The results obtained from the experience analytical method through taking the regional geological parameters and the hydrogeological parameters into empirical formulas and take the tunnel site area as a whole to study. But it is hard to determine the exact distribution of the water flow and the quantity of water by the above method. As we all know, most of accidents of the water inrush occurred in areas such as faults, joints and fissures. In order to predict the water inrush disaster more accurately, the present article attempt to construct a fracture network in the area of regional fault and joint surface. Then through the change of water flow in fracture we can predict where is the most likely area that the water inrush occurs.

In the study of simulating the water inrush by discrete fracture networks, the primary problem is how to construct the fracture network. To establish a reasonable fracture network, we first need to determine a three-dimensional fracture network model. With the on-going efforts of international scholars, the disk fracture network model [8], the polygonal fracture network model [9] and the circular pipe model [10] have been proposed in the past few years. After the fracture network model is constructed, then we should use the fracture networks model to simulate fracture distribution of the tunnel site. The Monte Carlo [11–13] simulation of fracture networks is widely used in the current methods of fracture network simulation. After the discrete fracture networks using the Monte Carlo method are defined, the related research about the calculation of the water inrush from the crack network can begin. Long and Min [14, 15] proposed a method for the seepage flow system and simulation of the fractured rock mass. The solution method for the characterization of the body element REV and the equivalent permeability coefficient and the method for determining the condition of using the equivalent continuum model are presented. The discrete fracture network model is based on the work of Long et al. [14]. Assuming that the permeability of the rock mass is not considered in the rock model. And according to the characteristics that water flow of every node in the fracture network is equal. The network model of the hydraulic head value and the permeability coefficient of the rock mass in the networks are constructed. After the discrete fracture network model is constructed, Min and Wilson [16, 17] has studied the seepage calculation of the two-dimensional fracture network, and a finite element calculation method for a two-dimensional fracture network has been proposed. Nœtinger [18] analysed the percolation model for three-dimensional fracture networks and proposed the use of the Darcy flow equation in three-dimensional fracture networks. Furthermore, to make the discrete fracture simulation become more efficient in the simulation, Cacas [10] proposed a method in which the crack is replaced with a conduit, thereby reducing the group number required to solve the equation by an order of magnitude. Dershowitz [19] proposed an optimization model that the polygonal fracture network was transformed into an approximate equivalent three-dimensional network consisting of a one-dimensional pipeline. And the water conductivity of the pipeline was deduced using the boundary element method [20]. Outstanding achievements have been made in the theoretical research of rock mass fracture network simulation, network optimization and seepage prediction and it has been applied in some fields. However, the application test case in actual tunnel project is relatively rare. Therefore, it is difficult to determine the degree of agreement between the theoretical analysis and the actual hydrogeological condition of tunnel. There is no comparison with the results obtained from the existing empirical method. And it is difficult to make a scientific evaluation for the practical of these theoretical methods in the tunnel water inrush. In this paper, combined with the previous research results, taking the Longmen Mountain tunnel as the research object, the discrete fracture network is constructed based on the Monte Carlo method. Then, this developed network is transformed into a three-dimensional pipe network model, combined with the Darcy flow equation and the analysis of the submergence. A prediction of water flow direction and water yield along the Longmen Mountain tunnel is made. And the results are compared with the predicted results using the commonly used precipitation infiltration and groundwater dynamics method. According to the water flow and water yield we can evaluate the possibility of water inrush along the tunnel and find out the dangerous place of water inrush.

2 Project introduction

2.1 Project overview

The Longmen Mountain tunnel passes through the Longmen Mountain area in northwestern Sichuan Province and is located at the junction of Mianyang City and the county of the Ngawa Tibetan and Qiang Autonomous Prefecture

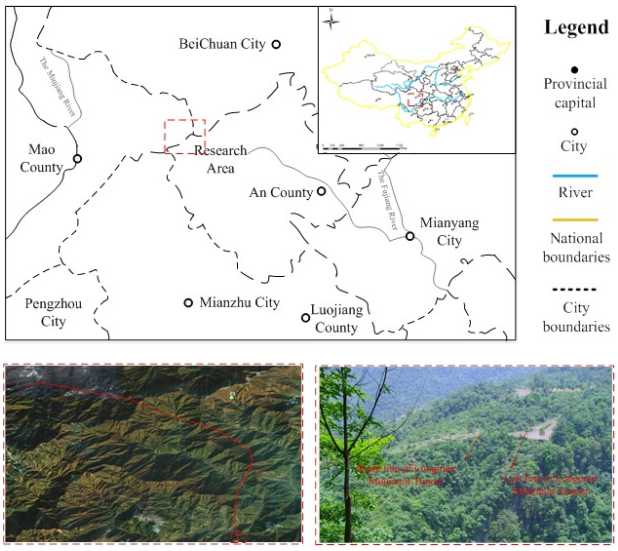

Figure 1: Longmen Mountain tunnel line position

in Maoxian. The start of the tunnel is the High-River station, and the tunnel continues to the Sheep-Ditch Bridge. The maximum line spacing of the tunnel is 60 m, and the minimum distance is 30 m. The mileage of the left line of the tunnel from the starting point to end is D2K91+020–D2K110+994.3, which covers a full length of 19,974.3 m, whereas the right line of the tunnel is YD2K91+002–YD2K111+046, covering a full length of 20,044.0 m. The Longmen Mountain Tunnel is a "cross-mountain" tunnel with a double line crossing the Longmen Mountain and the Fujiang River. "Cross-mountain" means the tunnel crosses the watershed (D2K104+160) upstream of the Tumen River (Jian-Jiang) and the Ju River (Luo Jiang) in the Fujiang River system in Sichuan Province. The tunnel has three transverse galleries, two shafts, one flat and three slag fields. The Longmen Mountain tunnel line position is shown in Figure 1.

2.2 Geological condition

The Longmen Mountain tunnel is located in the well-known Longmen Mountain structural belt, which is huge has a large-scale and complex structure. The overall trend is 45 degrees northeast with a northwest tendency. The tunnel stretches 500 km and has a width of 25–50 km. From east to west, there are 3 main faults: the former Longmen Mountain fault, the Longmen Mountain fault and the Longmen fault.

The Longmen Mountain tunnel passes through the central fault zone of Longmen Mountain. The central fault of the Longmen Mountain active structure is relatively intact, and aerial images of the linear features reveal a strong and active fault zone. The southwestern portion of the fault originates from the Luding and extends to the North East by Salt-wells, Ying show, Hongkou, Taiping, Beichuan, south of the dam and the Dam of Tea to the Shaanxi territory and the Mianxian-YangPingguan fault intersection, and the full length is 500 km. The overall trend is a 40N–60E fracture degree with a NW tendency and a 60–80 degree angle. The broken rock belt has a width of a few metres and is in the first hundred metres of the fault; the secondary faults are typically developed on both sides of the main faults, which are stacked in such a manner that shows that the extrusion thrusting has a right lateral strike slip property. According to the fracture activity differences and the geometric structure, the Longmen Mountain central fault is divided into four sections: the first is Yingxiu to the south, which is known as the Salt-Dragon fracture and late Pleistocene active segment; next is the Ying show-Nan Ba, which is referred to as the Yingxiu-Beichuan fault and has been active in the Holocene. the third is The Nan Ba to the Tea Ba, which is located in the western part of the Tea Ba-Lin-An temple fault and late Pleistocene active segment; the last one is the Tea Ba- Lin-An temple fault to the east has been active in the Middle Pleistocene. The tunnel cross section is within the Yingxiu-Beichuan fault, which follows the path from the town of Yingxiu in Wenchuan to the town of Mianzhu in Wang Jia Ping to the Qingping town line to the north and east of the counties of Lang Miao, Gao Chuan Xiang, and Beichuan, with a total length of 250 km, and is, throughout the entire Longmen Mountains, a "deep and large fault".

2.3 Hydrological conditions

The region of Longmen Mountain tunnel is in a subtropical humid monsoon climate characterized by a mild climate and four distinct seasons. The climate characteristics can be summarized as long winters and summers, little snow and rainfall, and little sunshine, with an annual average sunshine of 980.9 hours, which translates to 22% sunshine hours. The average temperature is 16.3 °C, with a frost-free period of 300.5 days, 1216.7 mm of mean annual evaporation, an annual average relative humidity of 77%. Over the past 34 years, the average annual precipitation has been 1167.87 mm (Table 1). The rainfall is mainly concentrated in 4 months: June, July, August and September (Figure 2).

The main water system in the study area includes the Tumen River, the Jinxi Gully and the Ju River, all of which belong to the Fu River system. The Tumen River and its

Table 1: Average rainfall statistics of An County

Rainfall Data \ Month	Jan.	Feb.	Mar.	Apr.	May.	Jun.	Jul.	Aug.	Sep.	Oct.	Nov.	Dec.
Early	2.8	5.0	7.0	13.6	22.7	27.8	61.3	96.3	79.0	27.7	9.5	2.0
Mid	2.8	7.8	10.8	14.2	30.3	46.9	89.6	121.6	59.3	22.8	6.5	2.2
Late	7.0	9.4	11.3	26.1	22.3	66.3	113.2	88.3	35.7	10.7	5.5	2.6
Average	12.6	22.2	29.1	53.9	75.3	141.0	264.1	306.2	174.0	61.2	21.5	6.8

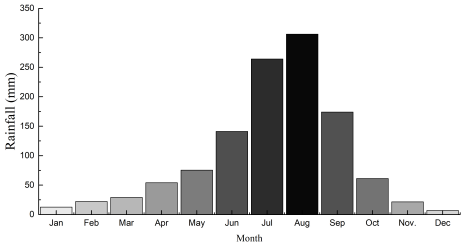

Figure 2: Average monthly rainfall histogram of An-County

tributaries to the north of the Longmen Mountains belong to the two tributaries of the Panjiang River, the three tributaries of the Fujiang River, and the so-called Horseshoe Creek. The Jinxi Gully and the Ju River are located south of the Longmen Mountains. The Xiao Ba hydrologic station measured an average flow of 11.4 in the Jinxi gully, whereas the Ju River has an average flow of approximately 10.58.

3 Fracture simulation and water inrush prediction

Because the fracture networks cannot be obtained from field measurements, there are difficulties in further studying water flow and water yield. Many researchers have found that although the geometric system of the discrete fracture network system is complex, its distribution characteristic is in accordance with a statistical distribution. Therefore, based on which, domestic and foreign scholars have extensively studied the distribution dynamics of the fracture networks. The basic research idea is to obtain the field structure fracture data then use a large number of experiments to verify these data. By analysing the parameters of the fracture, we have been able to make several conclusions: the crack openings follow a log-normal distribution [10], the crack length follows a power law distribution [21], and the fracture attitude follows a Fisher distribution [22], a Bingham distribution and so on. Based on the premises above, the three-dimensional discrete network model of the Longmen Mountain area was simulated using the Monte Carlo simulation method and was transferred to the network model. Then, a submerged analysis was employed with a surface area DEM, which was used to obtain the water area, and then combined with the Darcy flow equation to predict the water inrush in the tunnel.

3.1 Three-dimensional simulation of fracture

In the three-dimensional fracture simulation, the Monte Carlo method, which has been used extensively, was adopted to simulate the discrete fracture networks in three-dimensional. The three-dimensional network simulation of the discrete fracture of the surrounding rock was a complete set of the model system. The system is primarily composed of the geometric features of the discontinuous fracture surface, which is a type of geometric simulation. The system is primarily composed of the fracture surface properties, size, density, spacing, trace length and other simulations of the area of interest. Firstly, we needed to evaluate and analyse the surface fracture outcrop section. Then, the Monte Carlo simulation method was used to simulate the three-dimensional space. After the initial construction of the fracture networks, the discrete fracture network was transformed to a pipe networks model to facilitate the calculation of the seepage value. Then, the water inrush of the Longmen Mountain tunnel was predicted using the submerged analysis and the Darcy flow equation. In short, the Monte Carlo method was used to carry out a three-dimensional simulation, and the analysis of fracture water inrush employed the following several primary steps (Figure 3).

Step 1: Collection and processing the exposed data from the study surface area using photogrammetry, remote sensing and other means of surveying and mapping;

Step 2: Constructing a Monte Carlo simulation model to spatially simulate the location of the crack disk in the study area;

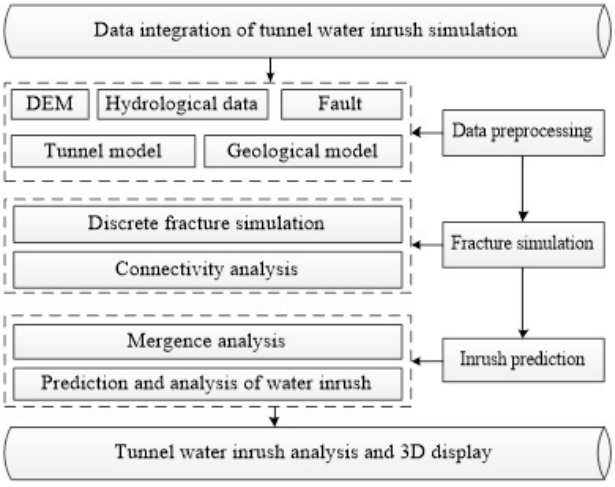

Figure 3: Algorithm flow chart

Step 3: Reasonably simulating the fracture trace length, spacing, density, yield and so on based on the joint sampling data;

Step 4: Comprehensively constructing a three-dimensional model of the discrete fracture network;

Step 5: Transforming the discrete fracture network model into a pipe network model;

Step 6: Introducing the inundation analysis, predicting the results of the water inrush in the Longmen Mountain Tunnel area based on the pipe networks model, and comparing the results with several common, currently used water inrush prediction methods.

According to the above process, first, we must obtain fracture sampling data. To obtain the preliminary fracture data, a certain method is applied. The common joint and fracture data collection method primarily includes endpoint coordinates of the exposed fracture areas, the shape and width of the surface, the filling material and the mechanical properties. To facilitate data collection and management, this paper constructs a local coordinate system. Typically, along the tunnel excavation direction, the midpoint of the lower tunnel starting point surface is the origin of coordinates, the tunnel excavation direction is defined as the horizontal axis, and the wall of the tunnel is set as the vertical axis to construct the local coordinate system (Figure 4).

A point fracture survey was designed considering above-mentioned joint fracture data. The joint and fracture investigation was carried out in the field. A number of joint and fracture data were collected and recorded in a survey table (Table 2).

Based on the above data, combined with the algorithm mentioned in this paper, a three-dimensional simulation of the discrete fracture network along the Longmen Mountain tunnel was conducted. Twenty-nine mileage segments were defined along the Longmen Mountain tunnel, and 19,990 fracture surfaces were simulated. Finally, the fracture value of the three-dimensional network model was generated using a simulation and is shown in Table 3.

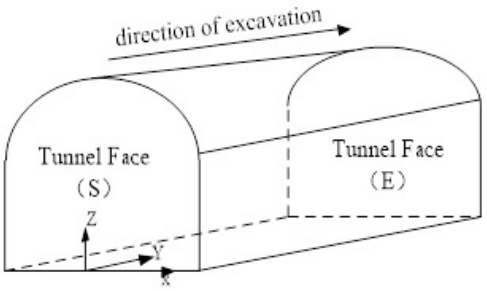

Figure 4: Local coordinate system of joint and fracture data acquisition

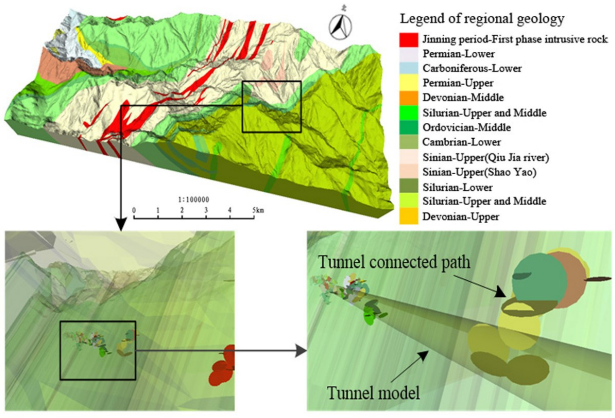

Figure 5: The discrete fracture networks connected path model in Longmen Mountain tunnel

After construction of the three-dimensional discrete fracture network, a depth-first traversal algorithm [23] was introduced to analyse the connectivity of the fracture network in the Longmen Mountain tunnel. Finally, the discrete fracture network connected path model (Figure 5) was obtained.

3.2 Water inrush prediction

3.2.1 The seepage water head

To assess the water inrush in the Longmen Mountain tunnel region, we first need to obtain the distribution of the surface water and groundwater in the area. The surface water is primarily caused by precipitation. However, the

Table 2: Joint and fracture survey of Longmen Mountain Tunnel

ID	End coordinates of joints						Attitude	width		Surface	mechanical
	x_1	y_1	z_1	x_2	y_2	z_2	dip	dip-angle	(mm)	morphology	
1	345.1	1.02	346.1	335.1	1.32	331.8	132	20	0.5	Dentate	Shear force
2	339.4	1.67	335.9	329.3	0.67	322.6	108	34	0.4	Straight	Shear force
3	341.8	1.71	337.6	311.5	1.91	331.2	74	29	0.3	Straight	Tension
4	345.4	1.33	316.3	345.1	1.13	325.6	66	38	0.3	Wavy	Shear force
...	...	...	...	...	...	...	...	...	...	...	...
290	185.2	12.02	80.1	174.4	9.23	71.4	80	23	0.2	Straight	Shear force
291	183.4	8.12	85.3	164.2	6.31	73.6	72	40	0.1	Dentate	Shear force
292	173.2	9.35	100.2	143.3	10.11	91.3	106	33	0.1	Straight	Tension
293	189.1	6.75	120.1	189.6	6.23	96.4	104	28	0.15	Wavy	Shear force
...	...	...	...	...	...	...	...	...	...	...	...
583	222.1	20.23	230.2	204.6	23.12	201.3	83	39	0.3	Dentate	Shear force
584	243.2	14.02	250.7	221.4	17.11	236.7	92	25	0.2	Straight	Tension
585	261.2	5.92	273.4	244.7	6.83	251.2	68	32	0.2	Straight	Shear force
586	283.2	2.02	280.1	274.5	2.21	291.4	110	35	0.3	Straight	Shear force

Table 3: Fracture networks simulation of Longmen Mountain Tunnel

ID	Centre position			Diameter	dip	dip angle
	x	y	z	(mm)	(°)	(°)
1	33.71641132	6.370506093	6.10342624	2.1	282.8	34.3
2	31.06662126	4.153187396	6.067980658	1.9	202.3	46.9
3	33.11070196	5.566152636	6.888274415	1.5	238.8	38.2
4	30.12239938	4.582461412	9.325489781	1.1	285.8	77.2
...	...	...	...	...	...	...
19989	20.88083148	8.820019606	5.948452045	4.4	140.4	59.4
19990	28.7655948	6.780095111	4.263190638	2.7	180.5	41.9

surface water does not cover the entire DEM but does cover most of the source water. Therefore, it is necessary, according to the existing water information combined with the presnet situation of the actual surface DEM. The connectivity of the actual surface DEM was analysised by the seed spread algorithm [24]. Finally, we can obtain the possible surface water storage location distribution. The water storage area is shown in Figure 6.

The surface water accumulation in the Longmen Mountain area can be obtained using a submerged analysis module based on the model of the seed spread algorithm. Then, we must calculate the water head value in these areas. Because most of the seepage occurs in the faults, joints and fractures, the permeability coefficient of surrounding rock and the seepage velocity are relatively high. Therefore, the time of the transient head [25] is not considered here. The values of seepage water head is shown in Table 4. The following formula can be used to estimate the transient head formed at the surface DEM due

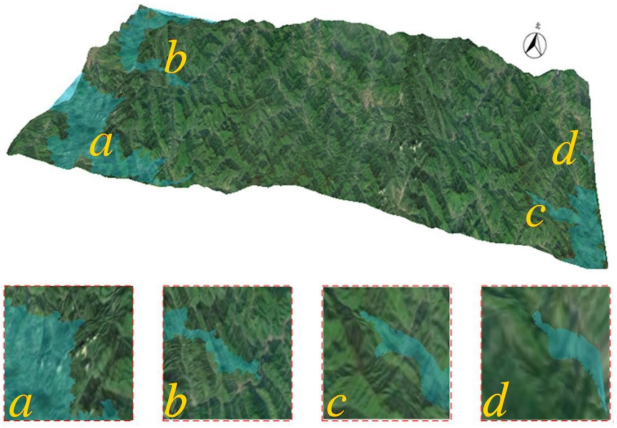

Figure 6: Water storage area

Table 4: The values of seepage water head

Subsection	Mileage		value of seepage water head (m)
1	D2K91+020	D2K91+560	381.5
2	D2K91+560	D2K91+700	173.1
3	D2K91+700	D2K93+440	2458.6
4	D2K93+440	D2K94+000	1582.6
5	D2K94+000	D2K94+060	226.1
6	D2K94+060	D2K94+450	1653.2
7	D2K94+450	D2K94+870	1978.2
8	D2K94+870	D2K94+980	647.6
9	D2K94+980	D2K96+250	3589
10	D2K96+250	D2K96+440	268.5
11	D2K96+440	D2K96+580	197.8
12	D2K96+580	D2K96+770	402.7
13	D2K96+770	D2K97+000	406.2
14	D2K97+000	D2K98+100	1942.9
15	D2K98+100	D2K98+690	1042.1
16	D2K98+690	D2K99+520	1466
17	D2K99+520	D2K100+850	2349.1
18	D2K100+850	D2K101+740	1572
19	D2K101+740	D2K102+610	1536.6
20	D2K102+610	D2K104+740	3762.1
21	D2K104+740	D2K105+060	565.2
22	D2K105+060	D2K105+170	233.1
23	D2K105+170	D2K107+220	3620.8
24	D2K107+220	D2K107+260	70.6
25	D2K107+260	D2K107+350	190.8
26	D2K107+350	D2K110+100	3885.8
27	D2K110+100	D2K110+150	106
28	D2K110+150	D2K110+994	1193

to the atmospheric rainfall:

$$h = \frac{q \times \lambda}{\phi} \tag{1}$$

In the formula h - transient head value;
q - average precipitation;
λ - infiltration coefficient of precipitation;
ϕ - porosity of the rock mass.

3.2.2 The water inflow capacity

After the water storage area and the head value are determined, a connected path of the three-dimensional network of the surrounding rock fracture needs to be obtained to analyse the water inrush of the tunnel line. According to the principle of the two-dimensional fissure flow model (Figure 7a), the connecting path of the three-dimensional fracture surface is transformed into a pipe networks model (Figure 7b), which is used to simulate the process along the tunnel path. The discrete network calculation method of the fracture network assumes that the surrounding rock is impervious. It is considered that the fluid flows only in the fracture and flows only along the direction of the lower water head in the connected fracture path. The theory of the network computing method is based on the balance of the flow at the intersection of each fracture surface. Then, the control equations of fracture network are established. An equation matrix with a series of related variables is obtained by solving the equation considered the hydraulic conductivity of a single crack. Finally, according to the given boundary conditions, we can obtain a solution to the equation.

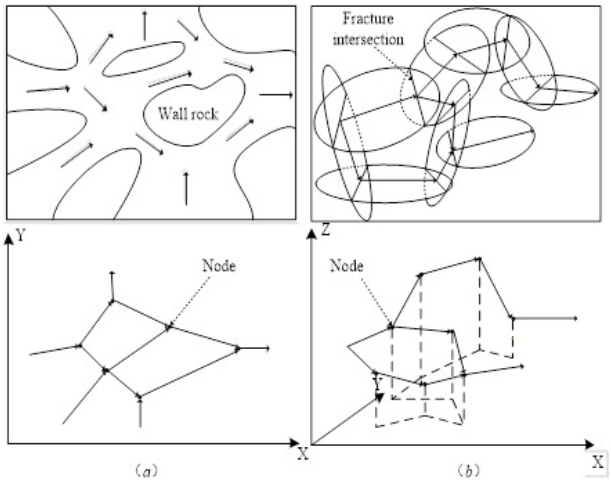

Figure 7: Fracture network transformation model

As shown in Figure 7, the discrete fracture disk is transformed into a pipe network model in three-dimensional space according to the above transformation. Next, this paper considers that water flows only in a fractured channel. The flow calculation is based on Darcy's Law Eq. (2):

$$\overline{u} = KJ \tag{2}$$

In this formula, $\overline{u}$ is the average flow velocity, J is the hydraulic gradient, and K is the permeability coefficient.

For linear flow motion in a parallel smooth crack, the average flow velocity in the crack can be obtained according to the principle of a hydraulic gradient and a viscous force balance.

$$v = \frac{b^2}{12}\frac{\rho g}{\mu}J = K_f J \tag{3}$$

In this formula, g is acceleration due to gravity, b is the crack width, μ is the dynamic viscosity coefficient of water, J is the hydraulic gradient, and K_f is the fracture permeability coefficient.

If the hydraulic gradient and the flow rate are nonlinear, the P. Forchheimer Eq. (4) is generally used:

$$J = av + bv^m \tag{4}$$

In this formula, a and b are given constants determined by the experiments, and 1.6<m<2. When an approximation is equal to 0, $m = 2$, the above formula can be changed into:

$$v = K_f J^{1/2} \tag{5}$$

On the basis of the formula, the method to determine the flow state according to the hydraulic gradient, which is the flow of water in the fracture, is proposed by Ломизе [26] (Table 5). Through an extensive number of experiments, the critical hydraulic gradient values corresponding to different fracture width b and a relatively coarse degree (for the absolute roughness of the fracture) were obtained (Table 5).

For the equations above, a given head value is required. In this paper, the initial water head values are given based on a condition in which the water area is obtained using the submerged analysis outlined above. According to the principle of the water flow equilibrium, the flow of each fracture segment to the common intersection point is zero or equal to the change of the flow rate at the intersection. The flow equation of node i can be obtained:

$$\sum_{i=1}^{n}(q_j) + Q_j = 0 \tag{6}$$

In this formula, is the flow of the j unit flow into or out of the intersection point i, n is the degree of the intersection point i, and Q_j is the source (sink) entry of intersection point i. The fracture network formula with n nodes can be transformed into n equations and transformed into a matrix form, as shown in Eq. (7):

$$Aq + Q = 0 \tag{7}$$

In this formula, $Q = (Q_1, Q_2, Q_3, \ldots, Q_n)^T$, $q = (q_1, q_2, q_3, \ldots, q_n)^T$, and $A = (a_{ij})_{n\times n}$ is the adjacency matrix of graphic model used in depth-first traversal algorithm in Section 3.1.

Simultaneously, the integral matrix form of the seepage calculation of the fracture networks is as follows Eq. (8):

$$(A \cdot Tl \cdot A^T)H + Q = 0 \tag{8}$$

In this formula, $Tl = \text{diag}\left(\frac{K_1 h_1}{l_1}, \frac{K_2 h_2}{l_2}, \frac{K_3, l_3}{l_3}, \ldots, \frac{K_n h_n}{l_n}\right)$.

In summary, the procedure used to solve the water head and flow at the intersection between the crack segment and the boundary for each crack section is as follows:

Step 1: Solve A^T according to the adjacency matrix formed by the fracture network A;

Step 2: Solve matrix T_1 according to the above formula;

Step 3: Derive the matrix equation after solving A, A^T and T_1;

Step 4: Insert the first and second boundary conditions into the equation to solve the water head value at the intersection point of the fracture;

Step 5: Calculate the seepage flow according to the head value of the fracture intersection point.

4 Results and discussion

This algorithm was primarily applied to the Longmen Mountain area where the tunnel is located. The algorithm uses the Monte Carlo method is used to study the three-dimensional simulation of discrete fracture network in the tunnel area. And subsequently we introduced the network model, flood analysis and Darcy flow equations to predict water inrush in the study area. The results were then compared with several commonly used methods to predict the tunnel water inrush. The water inflow results are shown in the following tables (Tables 6, 7 and 8):

Based on the results of the water inflow, we used the above water inflow in the curve (Figure 8) and three-dimensional effects graphs (Figure 9, 10 and 11). As shown in the figures, the green areas represent a lower possibility of water inrush, whereas the red areas indicate a higher possibility of water inrush. An increase in the depth of the colour indicates that water inrush probability gradually increased.

The simulation results of the algorithm proposed in this paper are in agreed well with the results of the groundwater dynamics simulation and precipitation infiltration method simulation, and the simulation results agreed well with the results of measurement of water inrush in the real tunnel [27]. However, it is still challenging to further improve the errors in some areas. On the whole, the algorithm proposed in this paper solves the tunnel water inrush prediction problem to a certain extent. At the same time, based on the water inrush simulation and the expression of the three-dimensional model, we can intuitively understand the possibility of water inrush along the tunnel, which provides the basic information for tunnel construction guidance and further, more precise prediction.

Table 5: Critical hydraulic gradient (Ломизе)

Width \ Roughness	0	0.1	0.2	0.3	0.4	0.5
0.1 cm	2.520	1.445	1.354	1.299	1.228	1.118
0.2 cm	0.315	0.182	0.169	0.161	0.153	0.139
0.3 cm	0.039	0.054	0.050	0.048	0.045	0.041
0.4 cm	0.039	0.023	0.021	0.020	0.019	0.017
0.5 cm	0.020	0.012	0.011	0.010	0.010	0.009

Table 6: Calculation table of groundwater dynamic method

Subsection	Start mileage	Termination mileage	Length B (m)	Permeability coefficient K (m/d)	Depth: still water level to the tunnel H (m)	Influence Radius R (m)	Coefficient a	Seepage volume Q (m^3/d)
1	D2K91+020	D2K91+560	540	0.100	20	56.6	1.924	1920
2	D2K91+560	D2K91+700	140	0.200	50	316.2	1.728	1246
3	D2K91+700	D2K93+440	1740	0.080	120	743.6	1.731	12204
4	D2K93+440	D2K94+000	560	0.150	110	893.6	1.693	6355
5	D2K94+000	D2K94+060	60	0.250	100	1000.0	1.670	995
6	D2K94+060	D2K94+450	390	0.250	90	853.8	1.675	6028
7	D2K94+450	D2K94+870	420	0.350	70	693.0	1.671	7365
8	D2K94+870	D2K94+980	110	0.400	80	905.1	1.658	2365
9	D2K94+980	D2K96+250	1270	0.150	150	1423.0	1.675	17768
10	D2K96+250	D2K96+440	190	0.005	170	313.5	2.112	176
11	D2K96+440	D2K96+580	140	0.010	190	523.8	1.933	234
12	D2K96+580	D2K96+770	190	0.100	200	1788.9	1.682	2275
13	D2K96+770	D2K97+000	230	0.080	210	1721.5	1.692	2344
14	D2K97+000	D2K98+100	1100	0.020	230	986.6	1.803	3716
15	D2K98+100	D2K98+690	590	0.030	250	1369.3	1.753	2776
16	D2K98+690	D2K99+520	830	0.020	270	1254.8	1.785	3041
17	D2K99+520	D2K100+850	1330	0.030	300	1800.0	1.737	7393
18	D2K100+850	D2K101+740	890	0.020	340	1773.2	1.762	3802
19	D2K101+740	D2K102+610	870	0.030	350	2268.3	1.724	5381
20	D2K102+610	D2K104+740	2130	0.020	360	1932.0	1.756	9460
21	D2K104+740	D2K105+060	320	0.050	370	3182.9	1.686	3223
22	D2K105+060	D2K105+170	110	0.200	360	6109.4	1.629	3769
23	D2K105+170	D2K107+220	2050	0.020	340	1773.2	1.762	8757
24	D2K107+220	D2K107+260	40	0.080	340	3546.4	1.666	575
25	D2K107+260	D2K107+350	90	0.200	300	4647.6	1.635	2686
26	D2K107+350	D2K110+100	2750	0.002	300	464.8	2.215	1712
27	D2K110+100	D2K110+150	50	0.200	200	2529.8	1.649	1106
28	D2K110+150	D2K110+994	844.3	0.002	150	164.3	2.483	389

5 Conclusion

This paper primarily based on field survey data and field data sampling of the Longmen Mountain tunnel area and data collection and the application of related algorithms. And then analyse the geological structural characteristics, hydrogeology, joints and fractures and regional geological data of the Longmen Mountain tunnel area, the three-dimensional fracture networks was constructed by the Monte Carlo simulation method in the area along the Longmen Mountain tunnel. And the connected path between the fracture networks was obtained through an analysis of the relation of the structural plane and the connectivity analysis of the fracture network generated by the simulation. Based on these results, this paper introduced inundation analysis and a three-dimensional simulation was carried out to the surface water distribution in the area of the Longmen Mountain tunnel. At last, combined with the existing water inrush simulation method, the possibility for water inrush in the Longmen Mountain tunnel length was evaluated comprehensively. The results show that three-

Table 7: Calculation table of precipitation infiltration method

Subsection	Mileage		Infiltration coefficient: α	Catchment Area $A = L \times B$ (km^2) influence width B (km)	line length L(km)	Seepage volume (m^3/d)
1	D2K91 +020	D2K91 +560	0.3	2	0.54	1045.3
2	D2K91 +560	D2K91 +700	0.35	3	0.14	474.3
3	D2K91 +700	D2K9 3+440	0.3	4	1.74	6736.6
4	D2K93 +440	D2K94 +000	0.4	6	0.56	4336.2
5	D2K94 +000	D2K94 +060	0.4	8	0.06	619.5
6	D2K94 +060	D2K94 +450	0.4	9	0.39	4529.8
7	D2K94 +450	D2K94 +870	0.4	10	0.42	5420.3
8	D2K94 +870	D2K94 +980	0.5	10	0.11	1774.5
9	D2K94 +980	D2K96 +250	0.3	8	1.27	9833.9
10	D2K96 +250	D2K96 +440	0.2	6	0.19	735.6
11	D2K96 +440	D2K96 +580	0.2	6	0.14	542.0
12	D2K96 +580	D2K96 +770	0.3	6	0.19	1103.4
13	D2K96 +770	D2K97 +000	0.25	6	0.23	1113.1
14	D2K97 +000	D2K98 +1 00	0.25	6	1.1	5444.5
15	D2K98 +1 00	D2K98 +690	0.25	6	0.59	2734.3
16	D2K98 +690	D2K99 +520	0.25	6	0.83	4016.8
17	D2K99 +520	D2K100 +850	0.25	6	1.33	6436.6
18	D2K100 +850	D2K101 +740	0.25	6	0.89	4307.2
19	D2K101 +740	D2K102 +610	0.25	6	0.87	4210.4
20	D2K102 +610	D2K104 +740	0.25	6	2.13	10308.2
21	D2K104 +740	D2K105 +060	0.25	6	0.32	1548.6
22	D2K105 +060	D2K105 +170	0.3	6	0.11	638.8
23	D2K105 +170	D2K107 +220	0.25	6	2.05	9921.0
24	D2K107 +220	D2K107 +260	0.25	6	0.04	193.6
25	D2K107 +260	D2K107 +350	0.3	6	0.09	522.7
26	D2K107 +350	D2K110 +100	0.2	6	2.75	10647.0
27	D2K110 +10 0	D2K110 +150	0.3	6	0.05	290.4
28	D2K110 +150	D2K110 +994	0.2	6	0.8443	3268.8

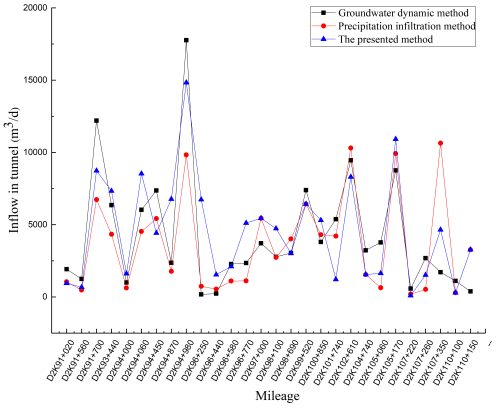

Figure 8: Comparison of the water inrush prediction curves

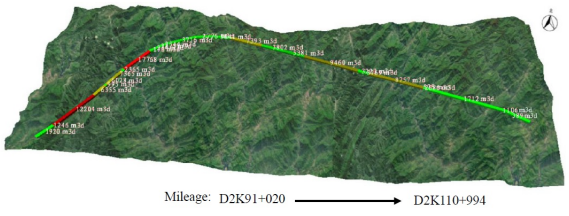

Figure 9: Prediction results of the groundwater dynamics method

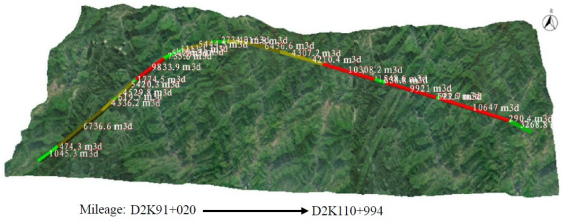

Figure 10: Prediction results of the precipitation infiltration method

Table 8: Algorithm prediction results in this paper

Subsection	Mileage		Infiltration coefficient, α	line length, L (km)	Seepage volume (m^3/d)
1	D2K91+020	D2K91+560	0.3	0.54	945.3
2	D2K91+560	D2K91+700	0.35	0.14	674.3
3	D2K91+700	D2K93+440	0.3	1.74	8736.6
4	D2K93+440	D2K94+000	0.4	0.56	7336.2
5	D2K94+000	D2K94+060	0.4	0.06	1619.5
6	D2K94+060	D2K94+450	0.4	0.39	8529.8
7	D2K94+450	D2K94+870	0.4	0.42	4420.3
8	D2K94+870	D2K94+980	0.5	0.11	6774.5
9	D2K94+980	D2K96+250	0.3	1.27	14833.9
10	D2K96+250	D2K96+440	0.2	0.19	6735.6
11	D2K96+440	D2K96+580	0.2	0.14	1542
12	D2K96+580	D2K96+770	0.3	0.19	2103.4
13	D2K96+770	D2K97+000	0.25	0.23	5113.1
14	D2K97+000	D2K98+100	0.25	1.1	5444.5
15	D2K98+100	D2K98+690	0.25	0.59	4734.3
16	D2K98+690	D2K99+520	0.25	0.83	3016.8
17	D2K99+520	D2K100+850	0.25	1.33	6436.6
18	D2K100+850	D2K101+740	0.25	0.89	5307.2
19	D2K101+740	D2K102+610	0.25	0.87	1210.4
20	D2K102+610	D2K104+740	0.25	2.13	8308.2
21	D2K104+740	D2K105+060	0.25	0.32	1548.6
22	D2K105+060	D2K105+170	0.3	0.11	1638.8
23	D2K105+170	D2K107+220	0.25	2.05	10921
24	D2K107+220	D2K107+260	0.25	0.04	93.6
25	D2K107+260	D2K107+350	0.3	0.09	1522.7
26	D2K107+350	D2K110+100	0.2	2.75	4647
27	D2K110+100	D2K110+150	0.3	0.05	290.4
28	D2K110+150	D2K110+994	0.2	0.8443	3268.8

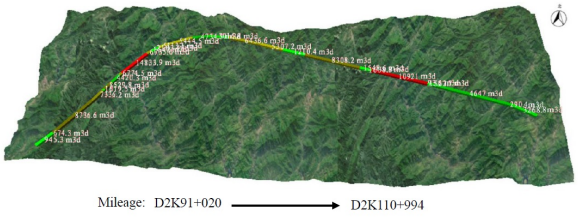

Figure 11: Prediction results of the presented method

dimensional simulation method of discrete fracture proposed in this paper can simulate the fracture distribution along the tunnel accurately. Based on this information, the possibility of the tunnel water inrush analysis mechanism can preliminarily predict the water inrush in the tunnel. The main research contents and conclusions of this paper are as follows:

1) Through the collection of the Longmen Mountain tunnel engineering geological data and the hydrogeological data, the topographic features, formation lithology, regional geological structure and subsurface hydrological characteristics of the study area were studied and analysed. The tunnel area was abundant in rainfall as it has a subtropical humid monsoon climate. The precipitation, landform, vegetation, development of weathering rock fis-

sures, and atmospheric precipitation, which is the main source of groundwater, create the conditions for water inrush.

2) Based on joint fracture sampling data and the relevant literature, a Monte Carlo simulation method along with the fracture simulation fissure structural plane was used. Then, the connected path in the fracture network was found through a preliminary screening using bounding boxes. Subsequently, we determined the structural plane relation and constructed the graph theory adjacency matrix model. Finally, we determined the path of the discrete fracture network using the depth traversal algorithm.

3) Through the analysis of the water inflow in a standard tunnel combined with the fracture network communication path, submerging analysis and other methods, the potential for water inrush in the Longmen Mountain tunnel was predicted using the proposed approach, the traditional groundwater dynamics method and the precipitation infiltration method separately. The prediction results were displayed in a three-dimensional framework.

Acknowledgement: This research was jointly supported by the Liaoning Province Natural Science Foundation (2015020581), the Fundamental Research Funds for the Central Universities (N140104002), the Key Project of Chinese National Programs for Fundamental Research and Development (2013CB036005), China Postdoctoral Science Foundation (2017M61181), National Natural Science Foundation of China (51609129), Shandong Postdoctoral Innovation Project Special Foundation (201502025) and State Key Laboratory for GeoMechanics and Deep Underground Engineering, China University of Mining & Technology (SKLGDUEK1515).

References

[1] Einstein, H.H., Risk and risk analysis in rock engineering. Tunnelling and Underground Space Technology. 1996,11(2), 141-155.

[2] Sturk, R. Olsson, L. Johansson, J., Risk and decision analysis for large underground projects, as applied to the Stockholm Ring Road tunnels. Tunnelling and Underground Space Technology. 1996,11(2), 157-164.

[3] Zarei, H.R., Uromeihy, A., Sharifzadeh, M., Evaluation of high local groundwater inflow to a rock tunnel by characterization of geological features. Tunnelling and Underground Space Technology. 2011,26, 364-373.

[4] Li, S.C; Zhou, Z.Q; Li, L.P., Risk assessment of water inrush in karst tunnels based on attribute synthetic evaluation system. Tunnelling and Underground Space Technology. 2013,38, 50-58.

[5] Zhao, Y.; Li, P.; Tian., S. Prevention and treatment technologies of railway tunnel water inrush and mud gushing in China. Journal of Rock Mechanics and Geotechnical Engineering. 2013,5, 468-477.

[6] Goel, R.K., Tunnelling through weak and fragile rocks of Himalayas. International Journal of Rock Mechanics and Mining Sciences. 2014,24, 783-790.

[7] Hwang, J.H; Lu, C.C., A semi-analytical method for analyzing the tunnel water inflow. Tunnelling and Underground Space Technology. 2006,22,39-46.

[8] Long, J.C.S., Gilmour, P., Witherspoon, P.A., A model for steady fluid flow in random three-dimensional networks of disc-shaped fractures. Water Resources Research. 1985, 21, 1105–1115.

[9] Dershowitz, W.S.; Einstein, H.H.,1987. Three dimensional flow modeling in jointed rock masses. In Proceedings of the 6th ISRM Congress, Montreal, Canada, 30 August-3 September. International Society for Rock Mechanics. pp. 87-92.

[10] Cacas, M. C., et al., "Modeling fracture flow with a stochastic discrete fracture network: calibration and validation: 1. The flow model." Water Resources Research.1990,3,479-489.

[11] Huang, F.M., Analytical solutions for steady seepage into an underwater circular tunnel. Tunnelling and Underground Space Technology. 2010, 25,391-396.

[12] Cahal, J.R., Coupling analysis of unsteady seepage and stress fields in discrete fractures network of rock mass in dam foundation. SCIENCE CHINA Technological Sciences. 2011,54,133-139.

[13] Souche, L.A.; Kherroubi, J.; Rotschi, M.J. ,2012. Fracture Network Characterization Method. US Patent US8301427.

[14] Long, J.C.S.; Remer, J.S.; Wilson, C.R.; Witherspoon, P.A., Porous media equivalents for networks of discontinuous fractures. Water Resources Research. 1982,18, 645-658.

[15] Min, K.B., Jing, L., Stephansson, O., Determining the equivalent permeability tensor for fractured rock masses using a stochastic REV approach: method. and application to the field data from Sellafield, UK. Hydrogeological Journal. 2004,*12*, 497-510.

[16] Min, K.; Rutqvist, J.; Tsang, C.; Jing, L., Stress-dependent permeability of fractured rock masses: a numerical study. International Journal of Rock Mechanics and Mining Sciences. 2014, 41, 1191-1210.

[17] Wilson, C.R.; Witherspoon, P.A., Steady state flow in rigid networks of fractures. Water Resources Research. 1974,10, 328–335.

[18] Nœtinger, B., A quasi steady state method for solving transient Darcy flow in complex 3D fractured networks accounting for matrix to fracture flow. Journal of Computational Physics. 2015,283, 205-223.

[19] Dershowitz, W.S., Fidelibus, C., Derivation of equivalent pipe network analogues for three-dimensional discrete fracture networks by the boundary element method. Water Resources Research. 1999,35,2685-2691.

[20] Dershowitz, W.S.,1996. Rock mechanics approaches for understanding flow and transport pathways. In Proceedings of the ISRM International Symposium - EUROCK 96, Turin, Italy, 2-5 September; International Society for Rock Mechanics.

[21] Dverstorp, B.; Andersson, J. Application of the discrete fracture network concept with field data: possibilities of model calibration and validation. Water Resources Research. 1989,25, 540-550.

[22] Baghbanan, A., Jing, L., Hydraulic properties of fractured rock

masses with correlated fracture length and aperture. International Journal of Rock Mechanics and Mining Sciences. 2007, 44, 704-719.

[23] Tarjan, R., Depth-first search and linear graph algorithms. Society for Industrial and Applied Mathematics. 1972,14, 114-121.

[24] Zhao, X., Wang, Y., Hongyu, L.I., Design and implementation of seed spread algorithm for calculations of source flood submerge area based on DEM. Science and Technology Review. 2012,30, 61-64.

[25] Knowles, I., Le, T., Yan, A., On the recovery of multiple flow parameters from transient head data. Journal of Computational and Applied Mathematics 2004,169, 1-15.

[26] Lomize GM. Flow in Fractured Rock (in Russian). Gosemergoizdat, Moscow, 1951

[27] Lin Bu, Shucai Li, Shaoshuai Shi, Lipin Li, Yong Zhao, Zongqing Zhou, Lichao Nie, Huaifeng Sun, Application of the comprehensive forecast system for water-bearing structures in a karst tunnel: a case study. Bulletin of Engineering Geology and the Environment.2017, online, DOI: 10.1007/s10064-017-1114-4.